IET Microwaves, Antennas & Propagation

Research Article

IET Journals
The Institution of Engineering and Technology

Coupled-line trans-directional coupler with arbitrary power divisions for equal complex termination impedances

ISSN 1751-8725
Received on 14th June 2018
Revised 7th August 2018
Accepted on 22nd August 2018
E-First on 11th October 2018
doi: 10.1049/iet-map.2018.5432
www.ietdl.org

Hongmei Liu[1], Chenhui Xun[1], Shaojun Fang[1] ✉, Zhongbao Wang[1,2], Dong Liu[3]

[1]*School of Information Science and Technology, Dalian Maritime University, Dalian, Liaoning 116026, People's Republic of China*
[2]*School of Electronic Engineering, Beijing University of Posts and Telecommunications, Beijing 100876, People's Republic of China*
[3]*School of Marine Information Engineering, Hainan Tropical Ocean University, Hainan, 572022, People's Republic of China*
✉ *E-mail: fangshj@dlmu.edu.cn*

Abstract: In the study, a coupled line trans-directional (CL-TRD) coupler that allows for equal complex termination impedances with arbitrary power divisions is presented. It is composed of two pairs of coupled lines with an overall electrical length of 90°, two types of shunt capacitors and three pairs of short-circuited stubs. By adjusting the electrical length of each short-circuited stub, as well as the values of the shunt capacitors, arbitrary equal complex termination impedances and power divisions are achieved. Moreover, since capacitors are shunted between the coupled lines, the proposed CL-TRD coupler has an inherent feature of dc blocking. Design equations for the CL-TRD were derived using even–odd mode decomposition analysis. To validate the theory, several numerical examples extracted from the design procedure were listed. Eventually, two prototypes of the proposed CL-TRD coupler are fabricated, and experiments are carried out. The measured results indicate that the coupler is able to realise arbitrary power divisions for equal complex termination impedance with good matching and isolation.

1 Introduction

Quadrature couplers [1–3], which exhibit two 90° phase-difference outputs with perfect isolation and all ports matched, are frequently used in radio frequency and microwave systems, such as mixers, amplifiers [4], and beamforming networks [5, 6]. Depending on the relative location of the isolated port to the input port, directional couplers are categorised into three types, namely, co-directional (COD), contra-directional (CTD), and trans-directional (TRD) [7]. One of the implementations for the TRD coupler is by using periodically capacitor shunted coupled lines, which is called the coupled line TRD (CL-TRD) coupler [8]. Compared with the COD coupler (branch-line coupler for instance), the CL-TRD coupler features small footprints and wide bandwidth. While in comparison with the CTD coupler (e.g. coupled-line coupler), the CL-TRD can achieve tight coupling with weak coupled micro-strip lines. In addition, the CL-TRD coupler can allow decoupling the direct current patch between input and output ports, which makes connections with active circuits easier, eliminating some off-chip biasing circuits. Recently, improvements in CL-TRD coupler performances have been reported that are high directivity [9], size reduction [10], and different power divisions [11]. Several methods have also been studied on improving the performance of other microwave components by using the CL-TRD coupler, e.g. compact planar balun [12], rat–race coupler with an adjustable power dividing ratio [13], and miniaturised Schiffman phase shifter [14]. Nowadays, the function extensions of the CL-TRD coupler have been focused, including frequency tunable [15] and coupling reconfigurable [16].

With the advent of modern wireless communication technology, a substantial reduction in mass and volume is required by the communication systems. Two methods for the reduction are adopted. Reduce the size of each component itself [17, 18], or control the termination impedances of the components to decrease the total size of microwave-integrated circuits [19–22]. The termination impedances are, in general, of arbitrary real values, but if they are complex, the size reduction effect may be far more intensified because the input impedances of the power amplifiers or antennas are not always real [23]. In [24,25], branch-line couplers with one group of equal complex termination impedances are introduced. However, since these couplers [24, 25] belong to the COD coupler and are implemented by branch lines, they inherit the big footprint and narrow bandwidth of branch line couplers. Up to now, couplers with all ports terminated with complex impedances have not been reported.

In this study, a compact CL-TRD coupler with equal complex termination impedances and arbitrary power divisions is proposed. It is composed of coupled lines, shunt capacitors and short-circuited stubs. Since the shunt capacitors are loaded between the coupled line sections, the proposed CL-TRD coupler has an inherent feature of dc blocking and is possible to be realised on a single printed circuit board layer. In Section 2, the mathematical analysis of the proposed CL-TRD coupler is derived by the even–odd mode decomposition technology and the design equations are provided to calculate the circuit parameters. In Section 3, two prototypes were designed, fabricated and measured using the design formulas. One of them has an equal complex termination impedance of $(40-\mathrm{j}20)\ \Omega$ and has a coupling of 3 dB, while the other is terminated in equal complex impedances of $(60-\mathrm{j}30)\ \Omega$ with 6 dB coupling. The measured results are given and the applications are also discussed, whereas, the concluding remarks appear in Section 4.

2 Theoretical analysis

Fig. 1 depicts the schematic diagram of the proposed CL-TRD coupler terminated in equal complex impedances of Z_L, $Z_L = R_L + \mathrm{j}X_L$, where R_L should be greater than zero, while X_L is a real number including zero. The CL-TRD coupler is composed of two pairs of coupled lines with the overall electrical length of 90°, two types of shunt capacitors and three pairs of short-circuited stubs. The even- and odd-mode characteristic impedances of the coupled lines are denoted as Z_{1e} and Z_{1o}, respectively, while each pair of the coupled line has an electrical length of θ_1. One type of capacitor named as C_1 is shunted between two ends of the coupled lines, while the other capacitor C_2 is loaded between the middle of the coupled lines. Shunt short-circuited stubs with an electrical length of θ_2 are tapped to the two ends of the coupled lines. The middles of the coupled lines are tapped with short-circuited stubs having an electrical length of θ_3. The characteristic impedances for the three pairs of short-circuited stubs are identically defined as Z_1.

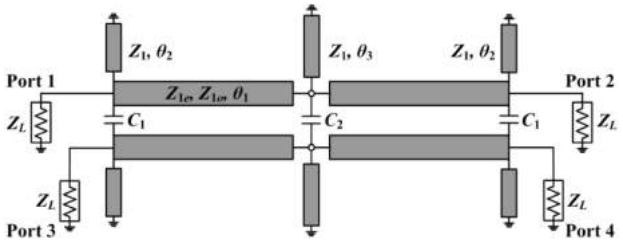

Fig. 1 *Schematic of the proposed CL-TRD coupler with complex termination impedances of Z_L*

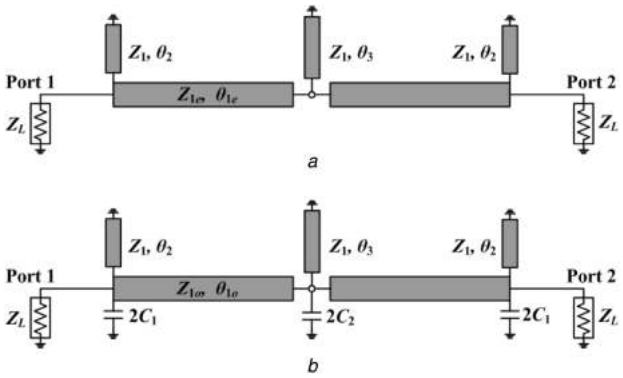

Fig. 2 *Equivalent sub-circuits of the proposed CL-TRD coupler with complex termination impedances of Z_L*
(a) Even-mode, ***(b)*** Odd-mode

Without loss of generally, if port 1 is designated as the input port, ports 3 and 4 are the coupled and through outputs, individually, and port 2 is the isolated port.

2.1 Design equations

Since the structure is symmetric across the horizontal axis, even–odd mode decomposition technique is utilised for analysing with the half circuits shown in Fig. 2. The scattering parameters (S_{11}, S_{21}, S_{31}, and S_{41}) of the CL-TRD coupler can be determined using reflection and transmission coefficients of the even- and odd–mode circuits [26]

$$S_{11} = \frac{1}{2}(\Gamma_e + \Gamma_o), \tag{1a}$$

$$S_{21} = \frac{1}{2}(T_e + T_o), \tag{1b}$$

$$S_{31} = \frac{1}{2}(\Gamma_e - \Gamma_o), \tag{1c}$$

$$S_{41} = \frac{1}{2}(T_e - T_o). \tag{1d}$$

In view of equal complex termination impedances, the $\Gamma_{(e,o)}$ and $T_{(e,o)}$ can be expressed using the ***ABCD*** parameters as

$$\Gamma_e = \frac{A_eZ_L + B_e - C_eZ_L^*Z_L - D_eZ_L^*}{A_eZ_L + B_e + C_eZ_L^2 + D_eZ_L}, \tag{2a}$$

$$\Gamma_o = \frac{A_oZ_L + B_o - C_oZ_L^*Z_L - D_oZ_L^*}{A_oZ_L + B_o + C_oZ_L^2 + D_oZ_L}, \tag{2b}$$

$$T_e = \frac{2\mathrm{Re}(Z_L)}{A_eZ_L + B_e + C_eZ_L^2 + D_eZ_L}, \tag{2c}$$

$$T_o = \frac{2\mathrm{Re}(Z_L)}{A_oZ_L + B_o + C_oZ_L^2 + D_oZ_L}. \tag{2d}$$

Referring to Fig. 2, the even- and odd-mode ***ABCD*** matrices of the proposed CL-TRD coupler are obtained as

$$\begin{aligned} A_{(e,o)} = {} & \cos 2\theta_{1(e,o)} - \frac{Z_{1(e,o)}b_{2(e,o)}}{2}\sin 2\theta_{1(e,o)} \\ & + Z_{1(e,o)}^2 b_{1(e,o)}b_{2(e,o)}\sin^2\theta_{1(e,o)} \\ & - Z_{1(e,o)}b_{1(e,o)}\sin 2\theta_{1(e,o)}, \end{aligned} \tag{3a}$$

$$B_{(e,o)} = \mathrm{j}Z_{1(e,o)}\begin{pmatrix} \sin 2\theta_{1(e,o)} \\ -Z_{1(e,o)}b_{2(e,o)}\sin^2\theta_{1(e,o)} \end{pmatrix}, \tag{3b}$$

$$C_{(e,o)} = \frac{\mathrm{j}}{Z_{1(e,o)}}\begin{pmatrix} 2Z_{1(e,o)}b_{1(e,o)}\cos 2\theta_{1(e,o)} \\ -Z_{1(e,o)}^2 b_{1(e,o)}^2\sin 2\theta_{1(e,o)} + \sin 2\theta_{1(e,o)} \\ +Z_{1(e,o)}b_{2(e,o)}\cos^2\theta_{1(e,o)} \\ -Z_{1(e,o)}^2 b_{1(e,o)}b_{2(e,o)}\sin 2\theta_{1(e,o)} \\ +Z_{1(e,o)}^3 b_{1(e,o)}^2 b_{2(e,o)}\sin^2\theta_{1(e,o)} \end{pmatrix}, \tag{3c}$$

$$D_{(e,o)} = A_{(e,o)}, \tag{3d}$$

where

$$b_{1e} = -Y_1\cot\theta_2, \tag{4a}$$

$$b_{2e} = -Y_1\cot\theta_3, \tag{4b}$$

$$b_{1o} = 2\omega C_1 - Y_1\cot\theta_2, \tag{4c}$$

$$b_{2o} = 2\omega C_2 - Y_1\cot\theta_3. \tag{4d}$$

To achieve TRD operation, as well as all-ports ideal matching ($S_{11} = S_{22} = 0$), and perfect isolation ($S_{21} = 0$), the following mathematical relations must be satisfied:

$$\Gamma_e = -\Gamma_o, \tag{5a}$$

$$T_e = -T_o. \tag{5b}$$

Then, the power division ratio k ($|S_{31}|/|S_{41}|$) of the proposed CL-TRD coupler can be expressed:

$$k = \frac{\left|A_eZ_L + B_e - C_eZ_L^*Z_L - D_eZ_L^*\right|}{2R_L}. \tag{6}$$

2.2 Parameter analysis

For compactness, the characteristic impedances of the short-circuited stubs (Z_1) are assigned to be equal with the even-mode characteristic impedance of the coupled lines Z_{1e}, and the phase coupling of the coupled lines is ignored. Since the overall length of the coupled lines is 90°, θ_1 is found to be 45°, and $\theta_{1e} = \theta_{1o} = \theta_1 = 45°$. Using the aforementioned conditions and substituting even-mode of (3) into (6), the expressions of Z_{1e} as functions of θ_2 and θ_3 are derived, as revealed in (7)

$$\begin{aligned} & Z_{1e}^2\left(1 + \frac{\cot\theta_3}{2}\right) + Z_{1e}X_L\begin{pmatrix} 2\cot\theta_2 + \cot\theta_3 \\ +\cot\theta_2\cot\theta_3 - \dfrac{2kR_L}{X_L} \end{pmatrix} \\ & -\left(R_L^2 + X_L^2\right)\begin{pmatrix} 1 - \dfrac{\cot\theta_3}{2} - \cot\theta_2\cot\theta_3 \\ -\cot^2\theta_2 - \dfrac{\cot^2\theta_2\cot\theta_3}{2} \end{pmatrix} = 0. \end{aligned} \tag{7}$$

It is observed from (7) that the curves of Z_{1e} versus θ_3 with different values of θ_2 can be plotted, and the values of Z_{1e} can be determined with proper values of θ_2 and θ_3.

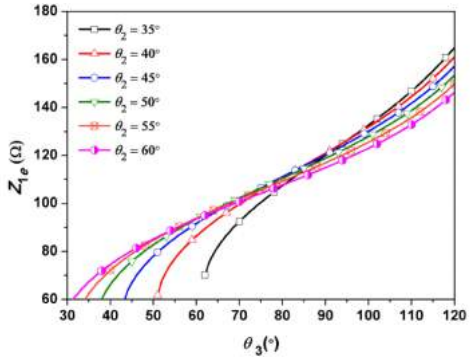

Fig. 3 *Z_{1e} versus θ_3 with different values of θ_2 (coupler A)*

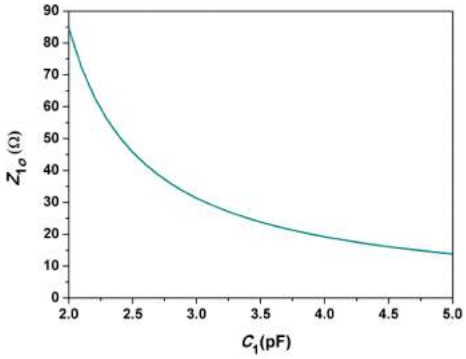

Fig. 4 *Curve of Z_{1o} versus C_1 (coupler A)*

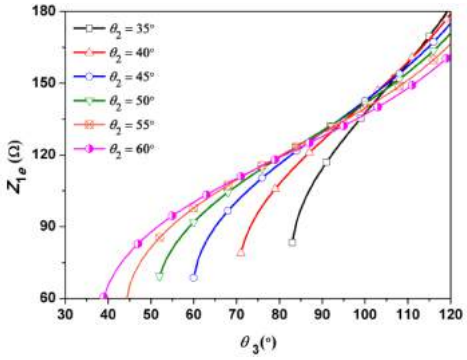

Fig. 5 *Z_{1e} versus θ_3 with different values of θ_2 (coupler B)*

Then, according to (5), the relations among even- and odd-mode ***ABCD*** matrices are found:

$$A_eR_L - 2C_eR_LX_L + D_eR_L = -A_oR_L + 2C_oR_LX_L - D_oR_L, \quad (8a)$$

$$2A_eX_L + B_e + C_e\left(R_L^2 - X_L^2\right) = -2A_oX_L - B_o - C_o\left(R_L^2 - X_L^2\right), \quad (8b)$$

$$2A_eX_L + B_e - C_e\left(R_L^2 + X_L^2\right) = 2A_oX_L + B_o - C_o\left(R_L^2 + X_L^2\right). \quad (8c)$$

Solving the three formulas in (8) simultaneously, the odd-mode characteristic impedance (Z_{1o}) can be calculated:

$$Z_{1o} = \frac{1 - g_2}{g_1 + (2\omega C_1 - Y_1\cot\theta_2)(1 - g_2)}, \quad (9a)$$

$$g_1 = \frac{C_eX_L^2 - 2A_eX_L - B_e}{R_L^2}, \quad (9b)$$

$$g_2 = g_1X_L - A_e + C_eX_L. \quad (9c)$$

Since the parameters (A_e, B_e, C_e, D_e) in the even-mode ***ABCD*** matrix can be calculated with obtained Z_{1e}, θ_2 and θ_3, the value of

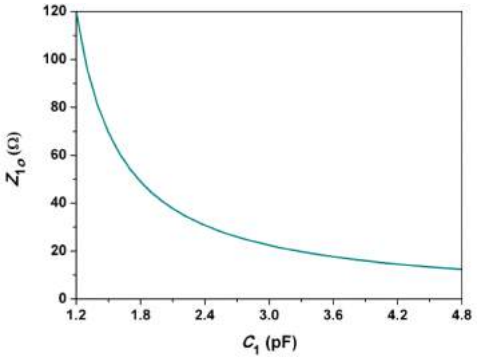

Fig. 6 *Curve of Z_{1o} versus C_1 (coupler B)*

Z_{1o} is varied with the capacitor C_1. Thus, Z_{1o} can be determined when a suitable value of C_1 is chosen.

Finally, the value of capacitor C_2 can be obtained using the following equation:

$$C_2 = \frac{1}{\omega}\left(\frac{g_2 + Z_{1o}(2\omega C_1 - Y_1\cot\theta_2)}{Z_{1o}(Z_{1o}(2\omega C_1 - Y_1\cot\theta_2) - 1)} + \frac{Y_1\cot\theta_3}{2}\right). \quad (10)$$

3 Design examples and procedure

In this section, two CL-TRD couplers are designed at 1.6 GHz to certify arbitrary power division and complex terminal impedances. The first one is 3 dB coupling for $Z_L = (40 - j20)\ \Omega$, named as coupler A, the second one is 6 dB coupling for $Z_L = (60 - j30)\ \Omega$, named as coupler B. The selections of even-mode characteristic impedance Z_{1e} and the capacitor C_1 will be investigated. The design procedure will also be provided.

3.1 Design of coupler A

According to the design requirements of coupler A (3 dB coupling, $Z_L = 40 - j20\ \Omega$), the values of k, R_L and X_L are 1, 40, and −20 Ω, respectively. From (7), the curves of Z_{1e} versus θ_3 with different values of θ_2 can be plotted, as shown in Fig. 3.

It is observed that the value of Z_{1e} is increased along with θ_3. While with the increasing of θ_2, the curve of Z_{1e} becomes more flatten. Considering size reduction, θ_2 and θ_3 are chosen as 45 and 50°, separately. The corresponding value of Z_{1e} is 77.9 Ω.

Then, according to (9), the curve of Z_{1o} versus C_1 can be obtained, as illustrated in Fig. 4. Since Z_{1o} should be less than Z_{1e} for the condition of coupled lines, C_1 is larger than 2.05 pF. Besides, for designing edge-coupled lines, a lower ratio of even- to odd-mode impedances is more favourable because the linewidth and gap required for fabrication are wider. Considering the fabrication constraints, Z_{1o} is chosen as 50.3 Ω, and the corresponding C_1 is 2.4 pF. Finally, C_2 is calculated as 2.92 pF from (10).

3.2 Design of coupler B

For coupler B, the coupling is 6 dB and the terminal impedance is $Z_L = 60 - j30\ \Omega$. Thus, $k = 0.58$, $R_L = 60\ \Omega$, and $X_L = -30\ \Omega$. Fig. 5 shows the curves of Z_{1e} versus θ_3 with different values of θ_2. In this design, θ_2 and θ_3 are chosen as 50° and 60°, respectively, the calculated value of Z_{1e} is 91.8 Ω. Fig. 6 reveals the curve of Z_{1o} versus C_1. In view of the fabrication limitation, Z_{1o} is chosen as 61 Ω, the corresponding values of C_1 and C_2 are 1.6 and 2.78 pF.

In summary, the design procedure of the proposed CL-TRD coupler is listed as below:

i. *Step 1:* Specify the power division ratio k and the complex termination impedances Z_L.

ii. *Step 2*: According to (7), the curves of Z_{1e} versus θ_3 with different values of θ_2 is plotted, and Z_{1e} can be determined with proper values of θ_2 and θ_3.

iii. *Step 3:* From (9), it is observed that Z_{1o} is a function of C_1. In view of fabrication constraints, the ratio of even- to odd-mode impedances should be <2. Thus, proper Z_{1o} is chosen, and the corresponding value of C_1 is obtained.

iv. *Step 4:* Substituting the known values into (10), C_2 can be calculated.

v. *Step 5:* Transform all the obtained parameters into physical dimensions and carefully optimise the model in electromagnetic (EM) simulation to obtain an improved performance.

Table 1 Several cases of the proposed CL-TRD coupler

Coupling, dB	Z_L, Ω	θ_2, °	θ_3, °	Z_{1e}, Ω	Z_{1o}, Ω	C_1, pF	C_2, pF
3	60 − j30	40	55	115.5	71.0	1.6	1.81
	40 − j20	45	50	77.9	50.3	2.4	2.92
	40 + j20	80	80	82.3	50.9	2.4	1.65
	60 + j30	80	70	107.4	72.6	1.6	1.09
6	60 − j30	50	60	91.8	61	1.6	2.78
	40 − j20	50	70	73.4	47.3	2.4	3.53
	40 + j20	90	80	65.1	44.5	2.4	3.02
	60 + j30	80	80	88.1	44.1	2.0	2.80
12	60 − j30	50	80	83.7	47.1	1.8	4.55
	40 − j20	45	80	49.1	32.3	2.7	5.87
	40 + j20	100	80	53.9	31.5	2.7	6.60
	60 + j30	90	80	74.4	48.3	1.8	3.96

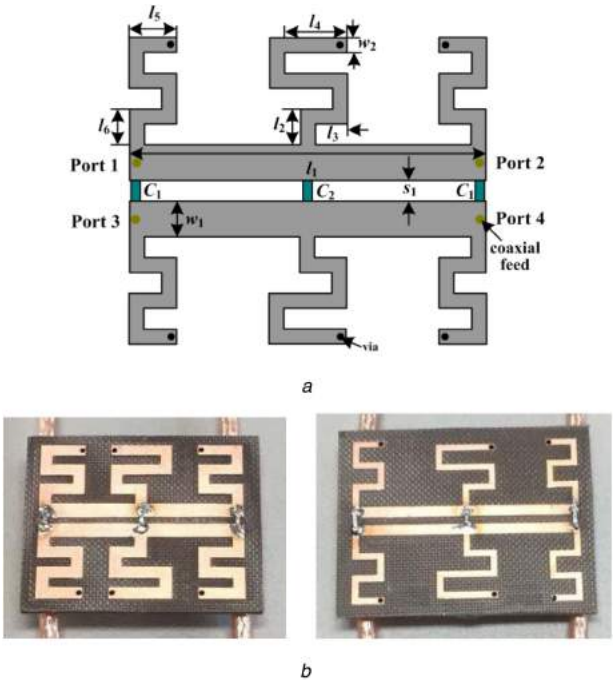

Fig. 7 *Fabricated proposed CL-TRD coupler*
(a) Layout, ***(b)*** Photographs

So far, the desired CL-TRD coupler with arbitrary power divisions and complex terminal impedances is prepared to be fabricated and tested based on the optimal dimensions.

3.3 Implementation and results

Using the aforementioned design theory and approach, several cases with different power divisions for different complex termination impedances were calculated in Table 1, including the circuit parameters of couplers A and B. To validate the proposed CL-TRD configuration, couplers A and B were implemented on the F4B substrate having dielectric constant $\varepsilon_r = 3.5$, dissipation factor $\tan\delta = 0.003$, substrate height = 1.5 mm. Fig. 7 shows the layout and photograph of the fabricated prototype. The short-circuited stubs are implemented by mender lines and the capacitors are GRM 1555 series (Murata, monolithic ceramic capacitors). The values of components and the main optimised dimensions of the designed structure are given in Table 2.

Since the couplers A and B are terminated in equal complex impedance, it is hard to measure it directly with a 50 Ω measurement system. To obtain the frequency responses with complex impedances, the couplers are firstly welded with the 50 Ω coaxial lines and then measured using 50 Ω termination impedances. The measured results are converted into those with the termination impedances by the Advance Design System with the de-embed method. Figs. 8 and 9 show the simulated and measured results for the couplers A and B, respectively.

For the coupler A, it is revealed from Fig. 8 that the measured input matching is 31.5 dB, and the output isolation is 36.3 dB at the defined operation frequency $f = 1.6$ GHz, indicating that there are a good return loss and high isolation in the fabricated prototype. Under the criterion of return loss (RL) >15 dB and isolation (IO) >15 dB, the operating bandwidth is from 1.36 to 1.74 GHz (23.75%). Small performance degradation could be due to the conductor loss, dielectric loss, fabrication errors or measurement errors. The measured coupling and insertion loss of coupler A is 3.0 and 3.4 dB, respectively. For amplitude imbalance <1 dB, the relative bandwidth is 21.25% (1.35–1.69 GHz). While from 1.36 to 1.73 GHz, the measured phase difference is 90° ± 5°.

Fig. 9 shows the simulated and measured results of the coupler B with a complex impedance of 60 − j30 Ω. It is observed that 32.2 dB input match and 38.1 dB output isolation is measured at the centre frequency. From 1.38 to 1.76 GHz, the measured return loss and isolation are both >15 dB. The measured bandwidth defined by 6.0 ± 0.5 dB coupling between the output ports is from 1.39z to 1.66 GHz. Also, in this frequency range, the measured phase difference is 90° ± 5°.

3.4 Application discussions

In this part, the applications of the proposed CL-TRD coupler will be further discussed. Firstly, consider the antenna applications. Since the input impedances (Z_a) of the power amplifier or low noise amplifier are not always real, if the proposed CL-TRD coupler is utilised, the amplifiers can be directly connected to the coupler when setting $Z = Z_a^*$. Also, the antenna will be designed with an input impedance of Z_L^*, as illustrated in Fig. 10. Thus, an active antenna can be realised with small size, low loss, and better performance.

Secondly, consider the microwave applications. If the termination impedances at ports 1 and 2 in Fig. 1 are denoted as Z_s,

Table 2 Values of components and the main optimised dimensions of the prototypes

Type	Coupler A	Coupler B	Type	Coupler A	Coupler B
w_1	1.9 mm	1.5 mm	l_4	6.2 mm	8.2 mm
w_2	1.5 mm	1.0 mm	l_5	5.7 mm	3.4 mm
s_1	0.8 mm	1.0 mm	l_6	2.75 mm	3.2 mm
l_1	25.5 mm	29 mm	C_1	2.4 pF	1.6 pF
l_2	2.75 mm	3.65 mm	C_2	3.0 pF	2.7 pF
l_3	3.1 mm	3.6 mm	r_{via}	0.35 mm	0.35 mm

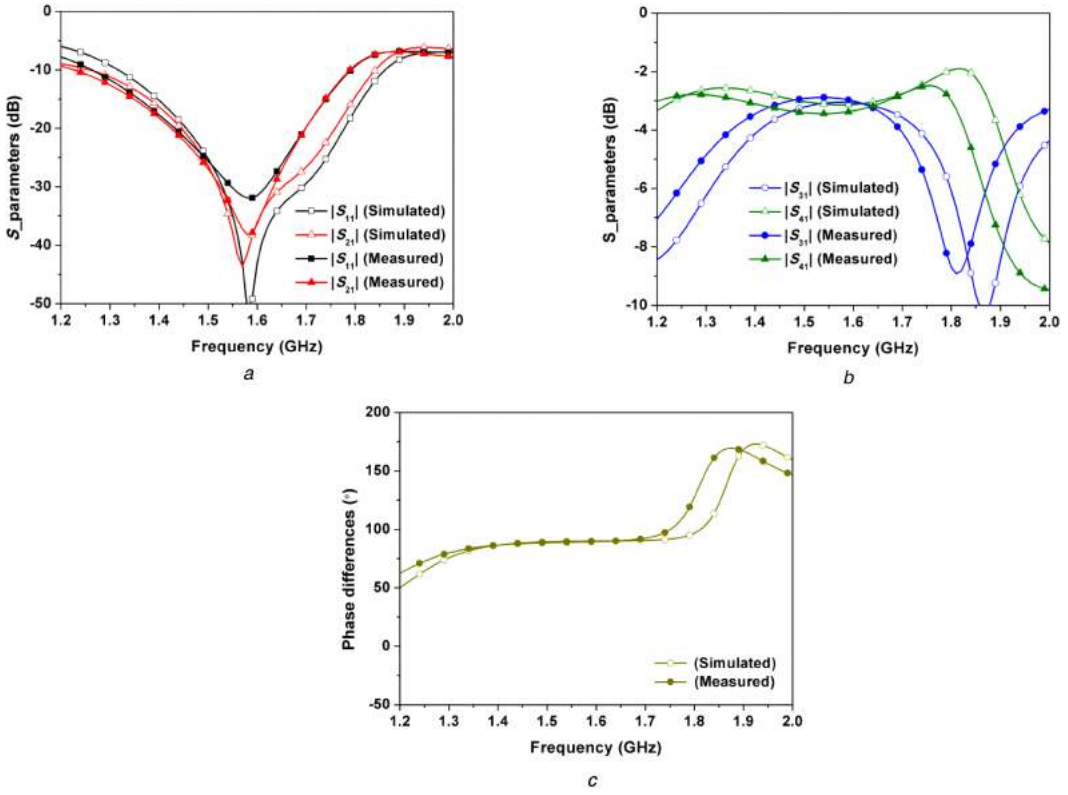

Fig. 8 *EM simulated and measured results of coupler*
(a) Matching and isolation, ***(b)*** Transmission, ***(c)*** Phase differences

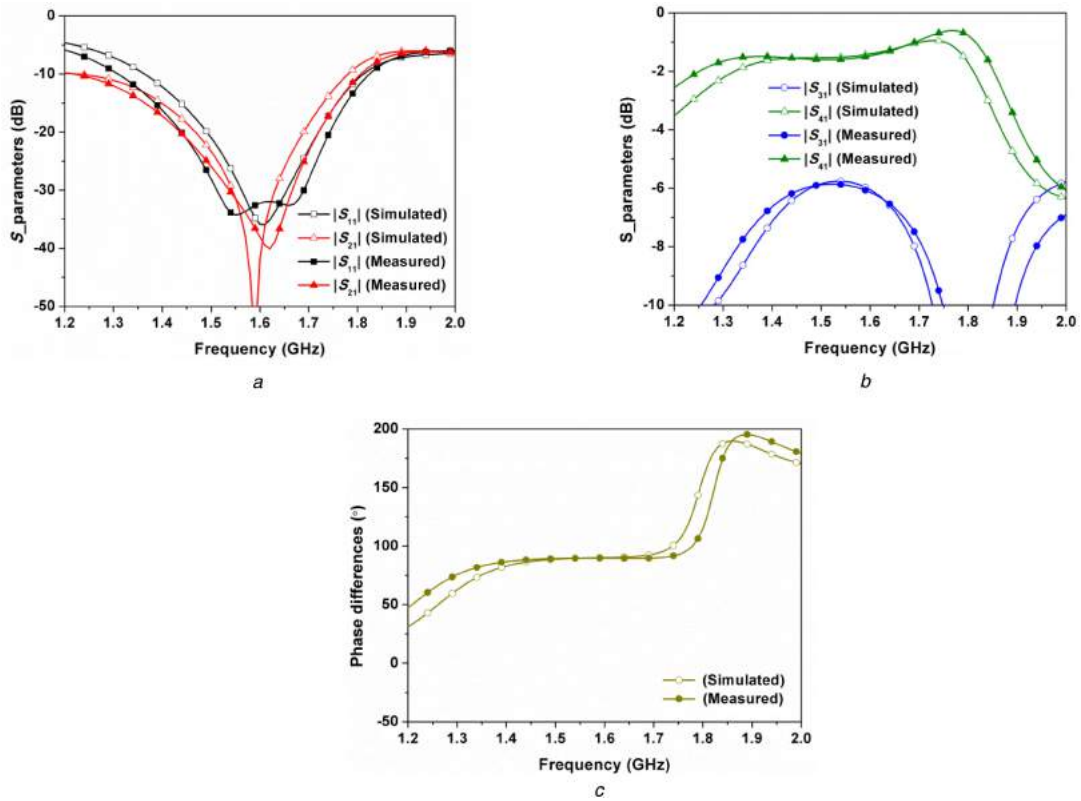

Fig. 9 *EM simulated and measured results of coupler B*
(a) Matching and isolation, ***(b)*** Transmission, ***(c)*** Phase differences

the study only investigates the case of $Z_S = Z_L$. In general, a coupler with $Z_S = 50\ \Omega \neq Z_L$ is desired. For the proposed CL-TRD coupler, this feature can be achieved simply by converting Z_L^* to $Z_S = 50\ \Omega$ by the method introduced in [23]. For example, if a 3 dB CL-TRD coupler with $Z_S = 50\ \Omega$ and $Z_L = (40 - j20)\Omega$ is wanted, a CL-TRD coupler with equal termination impedances of Z_L is firstly designed, as shown in Fig. 11*a*. Then, a coupler with $Z_S = 50\ \Omega \neq Z_L$ is constructed by simply adding an open stub to ports 1 and 2, as shown in Fig. 11*b* (the open stubs can be replaced by the capacitors, which has no influence on the circuit size). Since both CL-TRD couplers are designed at 1.6 GHz, all the circuit parameters are expressed as the values at 1.6 GHz and the

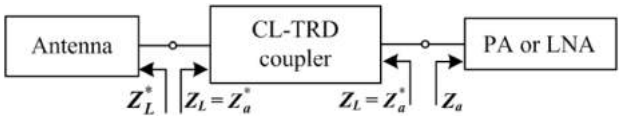

Fig. 10 *Block diagram for designing active antenna with the proposed CL-TRD couplers*

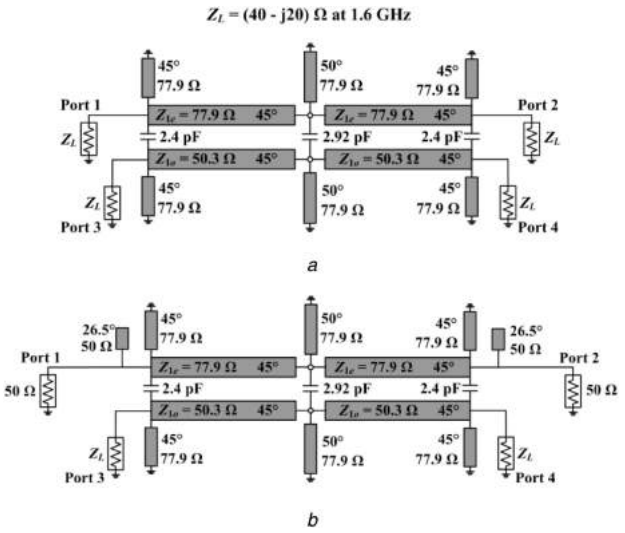

Fig. 11 *Two designed CL-TRD couplers*
(a) Equal termination impedances, ***(b)*** $Z_S = 50\ \Omega \neq Z_L$

capacitance value is that at 1.6 GHz as well. Fig. 12 shows the simulated results of the two types. One is with equal complex termination impedance (solid lines), and the other is with $Z_S = 50\ \Omega \neq Z_L$ (line with symbol). It is observed that the results of the two types of CL-TRD couplers are the same. Thus, the proposed structure can be applied in microwave applications.

4 Conclusions

In this study, a CL-TRD coupler with arbitrary power divisions for equal complex termination impedances is proposed. Analytical equations and rigorous design procedures are concluded as a guidance to simplify the design process. For demonstration, two experimental prototypes with 3 dB coupling for $40 - j20\ \Omega$ terminal impedances and 6 dB coupling for $60 - j30\ \Omega$ terminal impedances were fabricated and measured. The measured results are in agreement with the simulated ones, which indicated that the proposed structure can be utilised in microwave applications for size reduction and integration.

5 Acknowledgments

This work was supported in part by the National Natural Science Foundation of China under grant nos. 61571075, 51809030 and 61871417, in part by the China Post-Doctoral Science Foundation under grant nos. 2016T90066 and 2017M611210, in part by the Youth Science and Technology Star Project Support Program of Dalian City under grant no. 2016RQ038, in part by the Doctor Startup Foundation of Liaoning Province under grant no. 20170520150, in part by the Fundamental Research Funds for the Central Universities under grant nos. 3132016320 and 3132018183, and in part by the Scientific Research Project of Hainan University under grant no. Hnky2017ZD-17.

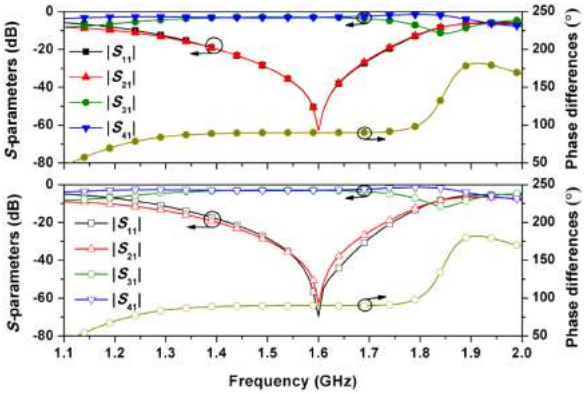

Fig. 12 *Simulated results of the proposed CL-TRD coupler with equal complex termination impedances (first figure) and with $Z_S = 50\ \Omega \neq Z_L$ (second figure)*

6 References

[1] Wang, L., Wang, G., Siden, J.: 'High-performance tight coupling microstrip directional coupler with fragment-type compensated structure', *IET Microw. Antennas Propag.*, 2017, **11**, (7), pp. 1057–1063

[2] Ting, H.L., Hsu, S.K., Wu, T.L.: 'Broadband eight-port forward-wave directional couplers and four-way differential phase shifter', *IEEE Trans. Microw. Theory Tech.*, 2018, **66**, (5), pp. 2161–2169

[3] Qamar, Z., Zheng, S.Y., Chan, W.S., *et al.*: 'Coupling coefficient reconfigurable wideband branch-line coupler topology with harmonic suppression', *IEEE Trans. Microw. Theory Tech.*, 2018, **66**, (4), pp. 1912–1920

[4] Jou, Z.J., Yang, Y., Chiu, L., *et al.*: 'A W-band balanced power amplifier using broadside coupled strip-line coupler in SiGe BiCMOS 0.13-μm technology', *IEEE Trans. Circuits Syst. I, Reg. Papers*, 2018, **65**, (7), pp. 2139–2150

[5] Wu, Q., Wang, H., Yu, C., *et al.*: 'L/S-band dual-circularly polarized antenna fed by 3-dB coupler', *IEEE Antennas Wireless Propag. Lett.*, 2015, **14**, pp. 426–429

[6] Jung, Y.K., Lee, B.: 'Dual-band circularly polarized microstrip RFID reader antenna using metamaterial branch-line coupler', *IEEE Trans. Antennas Propag.*, 2012, **60**, (2), pp. 786–791

[7] Vogel, R.W.: 'Analysis and design of lumped- and lumped-distributed element directional couplers for MIC and MMIC applications', *IEEE Trans. Microw. Theory Tech.*, 1992, **42**, (2), pp. 253–262

[8] Shie, C.I., Cheng, J.C., Chou, S.C., *et al.*: 'Trans-directional coupled-line couplers implemented by periodical shunt capacitors', *IEEE Trans. Microw. Theory Tech.*, 2009, **57**, (12), pp. 2981–2988

[9] Wang, Z.B., Liu, H.M., Fang, S.J., *et al.*: 'A novel 3-dB trans-directional coupler with DGS and conductor-backed asymmetric coplanar waveguides', *Frequenz*, 2013, **67**, (3–4), pp. 67–72

[10] Liu, H.M., Fang, S.J., Wang, Z.B., *et al.*: 'Miniaturization of trans-directional coupled line couplers using series inductors', *Prog. Electromagn. Res. C*, 2014, **46**, pp. 171–177

[11] Liu, H.M., Fang, S.J., Wang, Z.B.: 'Modified coupled line trans-directional coupler with arbitrary power divisions and its application to a 180° hybrid', *IET Microw. Antennas Propag.*, 2015, **9**, (7), pp. 1–7

[12] Shie, C.-I., Shie, J.-C., Chou, S.-C., *et al.*: 'Design of a new type planar balun by using trans-directional couplers', *IEEE Trans. Microw. Theory Tech.*, 2012, **60**, (3), pp. 471–476

[13] Wang, Z.B., Cao, Y., Fang, S., *et al.*: 'Miniaturized rat-race coupler with tunable power dividing ratio based on open and short circuited transdirectional coupled lines', *Microw. Opt. Technol. Lett.*, 2016, **58**, (11), pp. 2683–2689

[14] Cao, Y., Wang, Z.B., Fang, S.J., *et al.*: 'A miniaturized 90° Schiffman phase shifter with open-circuited trans-directional coupled lines', *Prog. Electromagn. Res. C*, 2016, **64**, pp. 33–41

[15] Liu, H.M., Fang, S.J., Wang, Z.B.: 'A compact trans-directional coupler with wide frequency tuning range and superior performance', *IEEE Trans. Compon. Packag. Manuf. Technol.*, 2017, **7**, (10), pp. 1670–1677

[16] Liu, H.M., Fang, S.J., Wang, Z.B.: 'Trans-directional coupler with adjustable coupling coefficients and reconfigurable responses', *IET Microw. Antennas Propag.*, 2017, **11**, (10), pp. 1340–1346

[17] Tang, C.W., Chen, M.G., Tsai, C.H.: 'Miniaturization of microstrip branch-line coupler with dual transmission lines', *IEEE Microw. Wirel. Compon. Lett.*, 2008, **18**, (3), pp. 185–187

[18] Kim, J., Yook, J.G.: 'A miniaturized 3 dB 90° hybrid coupler using coupled-line section with spurious rejection', *IEEE Microw. Wirel. Compon. Lett.*, 2014, **24**, (11), pp. 766–768

[19] Wu, Y.L., Wang, H.D., Zhuang, Z., *et al.*: 'A novel arbitrary terminated unequal coupler with bandwidth enhanced positive and negative group delay characteristics', *IEEE Trans. Microw. Theory Tech.*, 2018, **66**, (5), pp. 2170–2184

[20] Jiao, L.X., Wu, Y.L., Zhang, W.W., *et al.*: 'Design methodology for six-port equal/unequal quadrature and rat-race couplers with balanced and unbalance ports terminated by arbitrary resistances', *IEEE Trans. Microw. Theory Tech.*, 2018, **66**, (3), pp. 1249–1262

[21] Wu, Y.L., Zheng, S.Y., Leung, S.W., *et al.*: 'An analytical design method for a novel dual-band unequal coupler with four arbitrary terminated resistances', *IEEE Trans. Ind. Electron.*, 2014, **61**, (10), pp. 5509–5516
[22] Wu, Y.L., Jiao, L.X., Xue, Q., *et al.*: 'A universal approach for designing an unequal branch-line coupler with arbitrary phase differences and input/output impedances', *IEEE Trans. Compon. Packag. Manuf. Technol.*, 2017, **7**, (6), pp. 944–955
[23] Ahn, H.R., Nam, S.: '3-dB power divider with equal complex termination impedances and design methods for controlling isolation circuits', *IEEE Trans. Microw. Theory Tech.*, 2013, **61**, (11), pp. 3872–3883
[24] Pablo, A., Nuria, E., Luis, F.H., *et al.*: 'Complex impedance transformers based on branch-line hybrid coupler', *Prog. Electromagn. Res. C*, 2016, **69**, pp. 147–157
[25] Wu, Y.L., Shen, J.Y., Liu, Q., *et al.*: 'An asymmetric arbitrary branch-line coupler terminated by one group of complex impedances', *J. Electromagn. Waves Appl.*, 2012, **26**, pp. 1125–1137
[26] Pozar, D.M., Microwave Collin, R.E.: '*Foundations for microwave engineering*' (McGraw-Hill, New York, NY, USA, 1992, 2nd edn.)